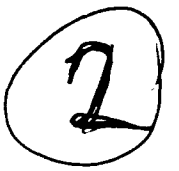

VERIFICATION AND CALIBRATION OF AN EDDY-RESOLVING MODEL OF THE GULF OF MEXICO

SAIC
Science Applications International Corporation
Report SAIC-91/1134
May 1991

James K. Lewis

Lakshmi Kantha

Artemio Gallegos

Ranjit Passi

Post Office Box 1303, 1710 Goodridge Drive, McLean, Virginia 22102, (703) 821-4300

VERIFICATION AND CALIBRATION OF AN EDDY-RESOLVING MODEL OF THE GULF OF MEXICO

James K. Lewis
Science Applications Int'l. Corp.
207 S. Seashore Avenue
Long Beach, Miss. 39560

Lakshmi Kantha
Naval Oceanographic and Atmospheric Research Laboratory
Stennis Space Center, Miss. 39529

Artemio Gallegos
Laboratorio de Oceanografia Fisica
ICMyL, UNAM
Mexico, D.F. 04510

Ranjit Passi
Institute for Naval Oceanography
Stennis Space Center, Miss. 39529

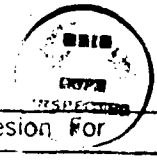

ABSTRACT

Techniques for verifying and calibrating an eddy-resolving ocean circulation model have been applied to a model of the Gulf of Mexico (GOM). Various kinematic parameters were calculated using drifter data from GOM Loop Current eddies, and indices of rotational period versus eddy age and swirl velocity versus distance from the eddy center were determined. The observed kinematics were then compared to the same parameters calculated from a model eddy. Although the model can simulate the movement and translation velocities of actual Gulf of Mexico eddies, it does not reproduce the interior flow characteristics of such eddies. In particular, the period of rotation about the center of a model eddy is considerably different from what is observed.

The first attempt at calibrating the model was the development of more realistic inflow conditions in the Yucatan Straits. A variety of data sets were synthesized to produce the two-dimensional distributions of temperature, salinity, density, and northward velocity as well as the east-west variations of surface height. The data of Cooper et al. (1990) was used to specify the vertical velocity profile while the results of Hall (1989) were used to specify the horizontal structure of the flow field. This synthesized profile was adjusted upward to give the 30 Sv that is typical of the Yucatan Straits inflow, an increase of only 7%. The results compare well with the limited observations of currents in the Yucatan Straits.

To obtain the density field, observed temperature and salinity fields at the Yucatan Straits were used to calculate water densities with depth along the western edge of the Straits. Geostrophy was then used to calculate the surface height variations and the mass field based on the newly synthesized velocity field. The equation of state and the T-S relationship were then used to construct the fields of temperature and salinity from the synthesized mass field. These synthesized fields compare well with the observed fields, implying that the flow through the Yucatan Straits is in near-geostrophic balance.

1. INTRODUCTION

Ocean models are now capable of reproducing some salient aspects of western boundary currents. In particular, such models can reproduce the broad features (if not the correct phase) of the meandering of such currents, eddy shedding, and eddy movement. We are now at a stage to use observations to verify characteristics of the currents and eddies of hydrodynamic models. Specifically, we can verify maximum current magnitudes, the vertical structure of the currents, the angular momentum (potential vorticity) of eddies, and the translation rate of eddies. If the above characteristics are not reliably reproduced, then we cannot expect the density structure of the water column in and around the western boundary current and its eddies to be well simulated by the model. This can be a

critical factor when the model density structure is used to determine noise propagation characteristics through the water column.

It is apparent that a series of steps should be formulated to provide a basis for verifying and calibrating eddy-resolving models. Verification comes in the form of comparing certain observed eddy and boundary current characteristics with those of the model eddies and current. Attributes which must be reproduced by the model are the maximum current speed, the horizontal and vertical structure of the currents, and the period of rotation for eddies. Such comparisons can then lead to improving the model's fit to observations by the adjustment of specific parameters of the model.

This study presents some preliminary results of the initial verification and calibrations for an operational, eddy-resolving model of the Gulf of Mexico (GOM). There is a wealth of eddy observations in the Gulf (Lewis and Kirwan, 1985, 1987; Lewis et al., 1989; Cooper et al., 1990) that has been used to assess how well the GOM model is performing and to improve the model. In addition, realistic model inflow conditions for the Yucatan Straits have been developed based on recent data and other research (Hall, 1989; Cooper et al., 1990).

Our initial analyses follow along the lines of Kirwan et al. (1990) which are based on water parcel path data from ocean drifters and from the model. The path data are used to determine various kinematic parameters of actual and model eddies (see Kirwan et al., 1984, 1990). Differences between the observed and model kinematic parameters are used to verify the model's ability to reproduce mesoscale phenomena in the ocean. As will be shown, although the GOM model can simulate the movement and translation velocities of actual Gulf of Mexico eddies, it does not reproduce the interior flow characteristics of such eddies. In particular, the period of rotation about the center of a model eddy is considerably different from what is observed.

2. ANALYSES OF OBSERVED GOM DRIFTER DATA

As the Gulf Stream enters the Gulf of Mexico through the Yucatan Straits, it can penetrate northward and develop a loop-like structure as it seeks its outflow through the Florida Straits. Thus, the Gulf Stream within the Gulf of Mexico is typically referred to as the Loop Current. Eddies that are shed from the Loop Current have often been seeded with drifters. The analysis technique of Kirwan et al. (1984, 1990) decomposes observed and model-simulated drifter trajectories into the basic kinematics of translation velocity of an eddy, amplitude of the swirl speed (rotation speed about the center of the eddy), vorticity, divergence, and deformation rates. The two parameter sets are then compared to assess the performance of the model.

Drifter Identification	Time in Gulf of Mexico
1599	19 Nov 1980-31 Mar 1981
3344	8 Nov 1987-20 May 1988
3345	16 May-31 Dec 1988
3347	20 Oct-31 Dec 1988
3350	29 Apr-15 Jul 1984
3354 (In Loop Current)	18 Jun-15 Sep 1985
3374	6 Oct 1982-10 Aug 1983
3378	18 Jul 1985-26 Jun 1986
3379	7 Mar 1986-22 Jan 1987
5495 (Two Eddies)	29 Jun 1985-23 Jan 1986

Table 1. Drifters and periods during which position data were collected.

The path data used in this study (Table 1) have been discussed in previous studies, specifically Kirwan et al. (1984), Lewis and Kirwan (1985, 1987), Lewis et al. (1989), and SAIC (1990). We have analyzed these data to provide information about individual Loop Current eddies as well as some overall general characteristics. Altogether, path data from 10 drifters were analyzed, one of which was in the Loop Current itself. Fig. 1 shows examples of the paths of two of these drifters. One

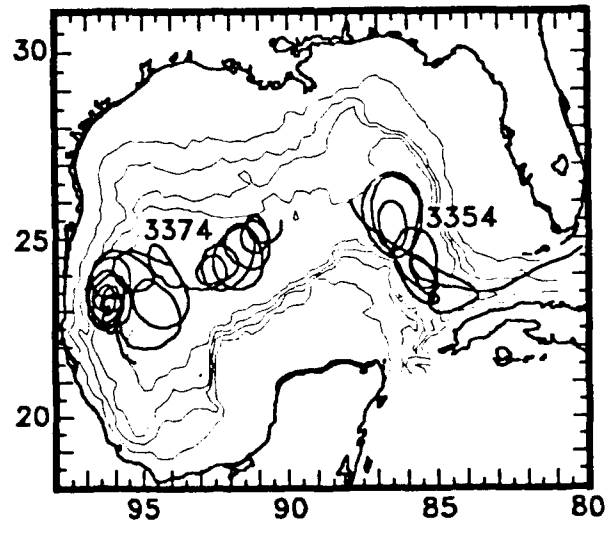

Fig. 1. Examples of drifter trajectories in the Gulf of Mexico. The drifter in the eastern Gulf (drifter 3354) was in the Loop Current and is discussed in Lewis and Kirwan (1987). The drifter in the western Gulf (drifter 3374) was in a westerly-migrating Loop Current eddy.

was from a Loop Current eddy that moved into the western GOM and then translated northward along the Mexican coastline, and the other was that drifter caught in the flow field of the Loop Current.

We present two examples of the analyses of the drifter data. The first is that of drifter 3345 (Fig. 2) which moved westward through the deepest waters of the Gulf. Although this path is the most common, it is possible for an eddy to take a more northerly route across the Gulf. The east-west (u) and north-south (v) velocity components of drifter 3345 are shown in Fig. 2. Note that there are low frequency variations in the magnitudes of the components, an indication of the eddy slowly diverging (speeds becoming greater) and converging (speeds becoming smaller). This phenomena is seen in all of the longer term path data. The results of the kinematic analysis are also shown in Fig. 2. The translation velocities clearly indicate the west-south-westward movement of the eddy, on the order of ~5 cm/s. The swirl velocities vary from 30-90 cm/s, with lower velocities associated with the drifter being closer to the center of the eddy. The drifter was as close as 50 km to the eddy center but moved out to ~110 km several times. The

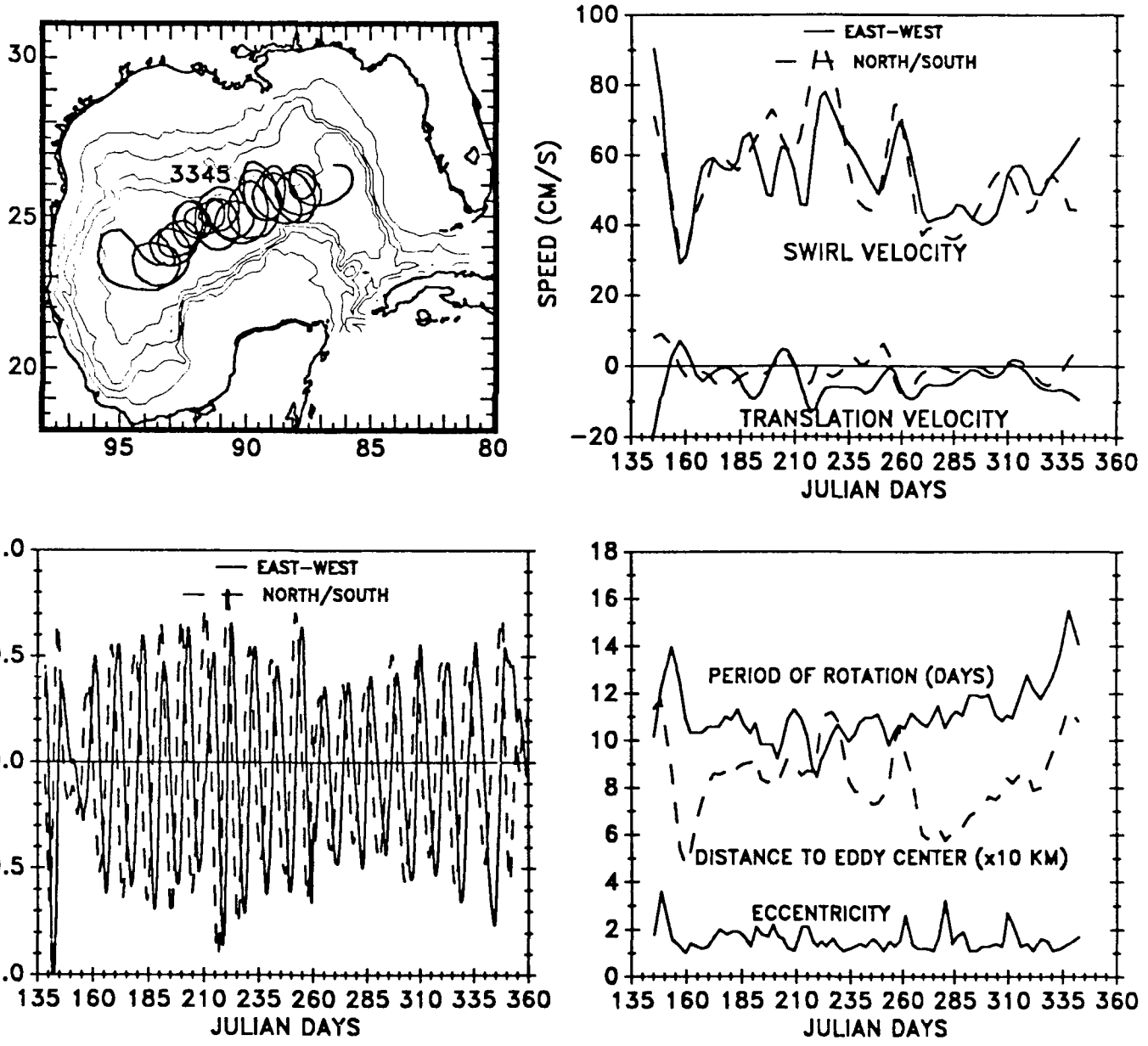

Fig. 2. Trajectory of drifter 3345 (top left), the east-west (u) and north-south (v) velocity components (bottom left), swirl and translation velocities (top right) and period of rotation, distance to eddy center, and eccentricity (bottom right).

SAIC

eddy rotation rate was fairly constant at ~11 days except at the end of the deployment when the period reached as high as 16 days. The data indicate that the eddy was not quite circular, with an average eccentricity (major axis length divided by the minor axis length) of ~1.75.

Drifter 1599 (Fig. 3) was in a ring which impacted the Mexican coast at about 23°N and then began migrating northward. The velocity component data shown in Fig. 3 again show variations in the magnitudes of the speeds. The curious speed variations seen in the v component during Julian days 390-420 occurred when the path of the drifter became highly elliptical, almost peanut-shaped. The peanut-shaped trajectory is quite typical, occurring when an approaching eddy begins to coalesce with an older eddy located along the Mexican coast. The translation velocities show the westward then northward movement of the eddy. Again, the rate of movement was about 5 cm/s. The swirl velocities varied from 10 to 70 cm/s. again dependent on distance from the eddy center, which varied from 25-105 km (Fig. 3). The rotation rate averaged about 12 days with the exception of the time when coalescing occurred. At the beginning of this process, the rotation rate nearly

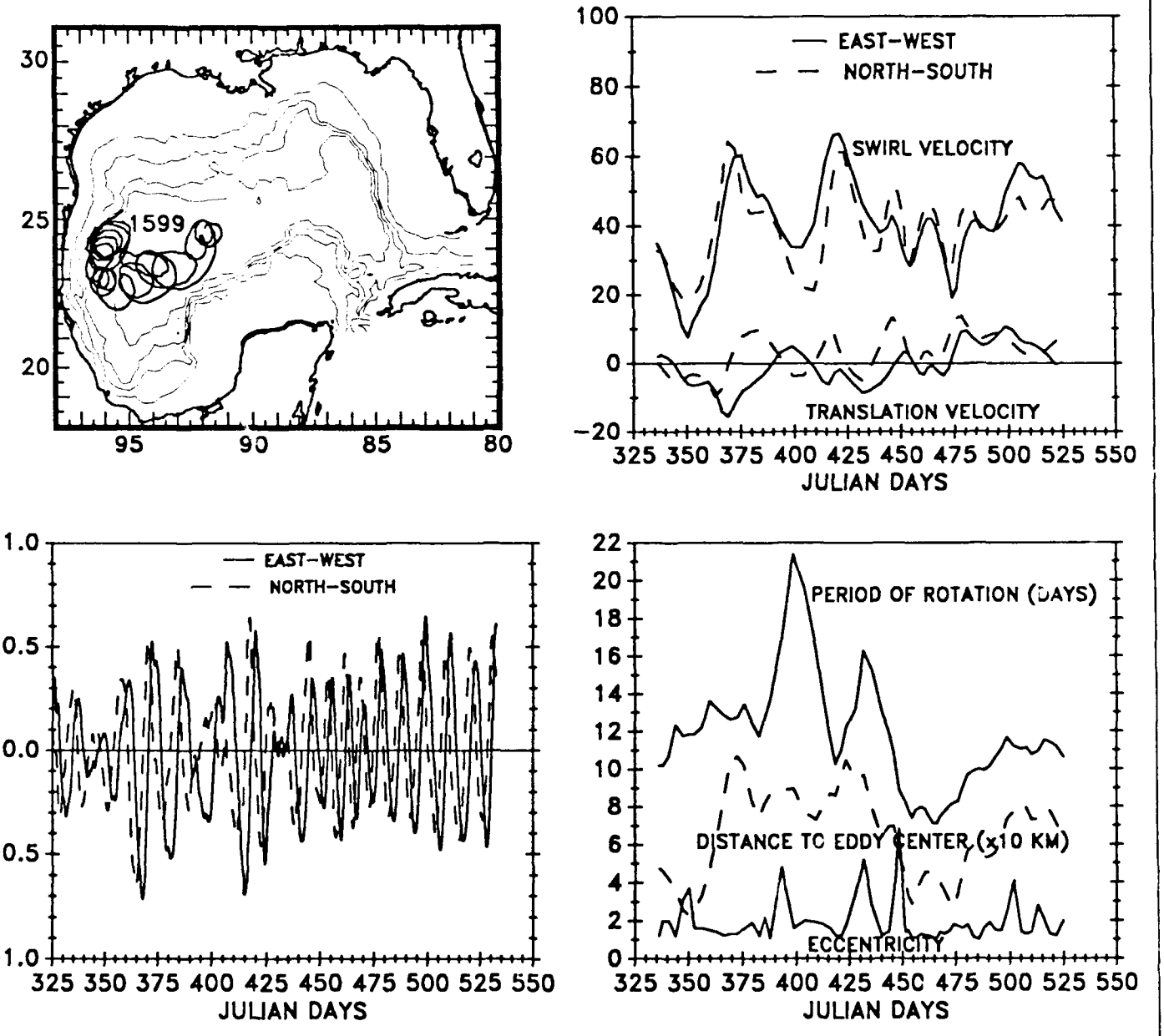

Fig. 3. Same as Fig. 2 but for drifter 1599.

SAIC

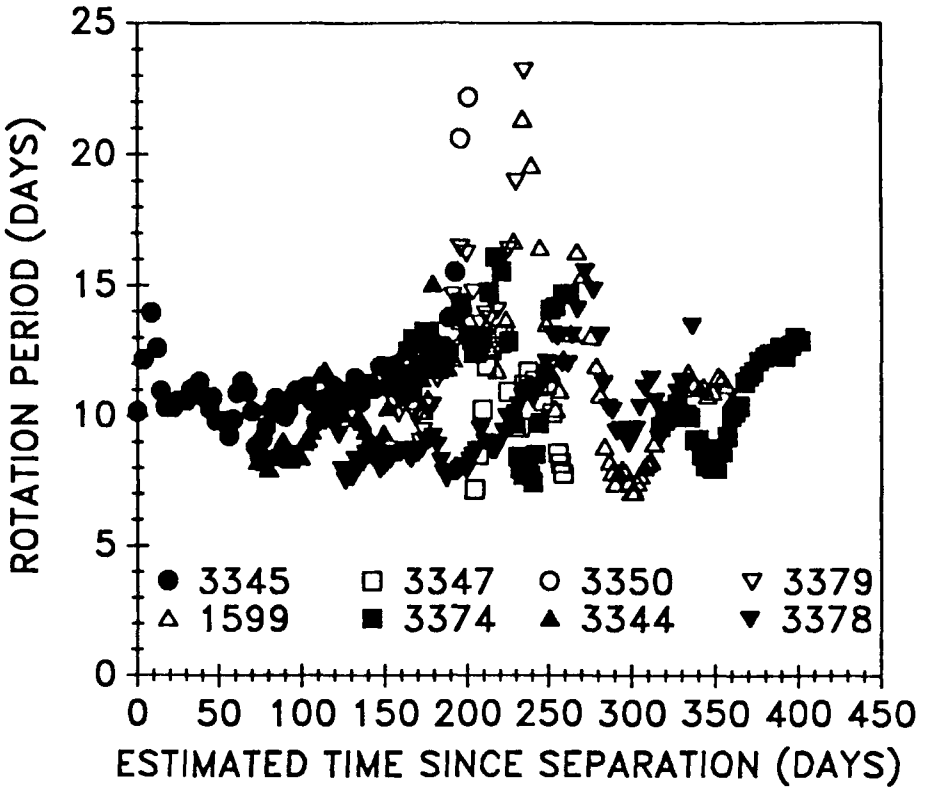

Fig. 4. Period of rotation for Loop Current eddies as determined from the path data from eight drifters.

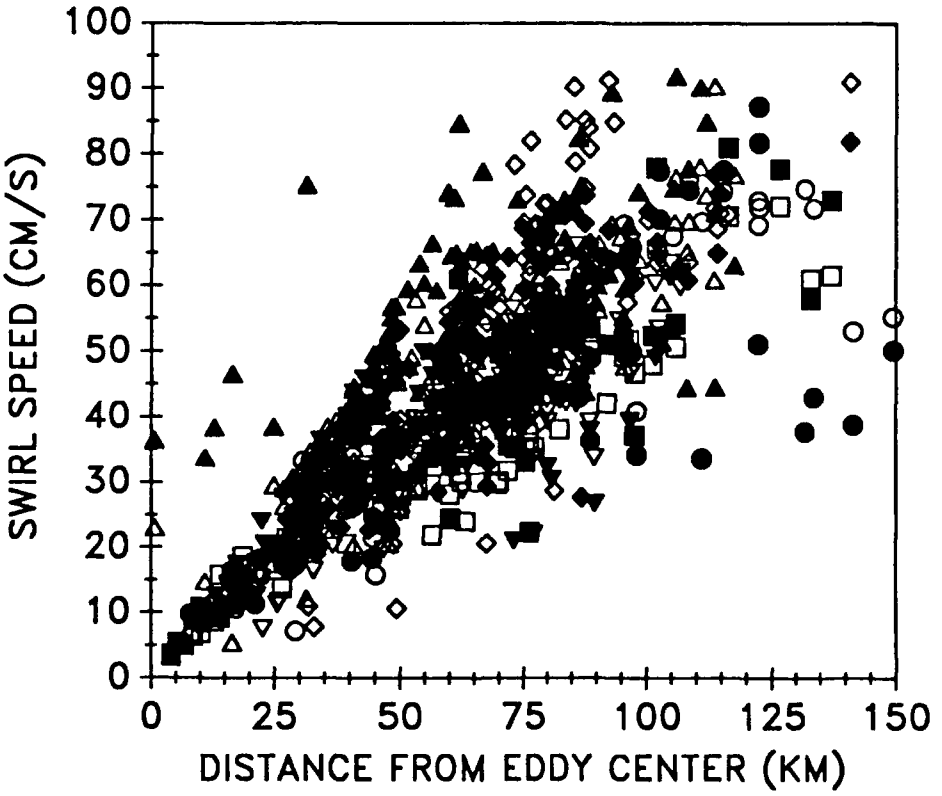

Fig. 5. Swirl speed vs. distance from the center of rotation for all drifter data.

SAIC

doubled, going up to ~23 days.

The results of all the analyses were used to develop two general indices of Loop Current eddy kinematics. The first of these is the period of rotation as a function of time since the eddy separated from the Loop Current. Since it is not always possible to estimate the exact time of eddy separation, we used the movement of drifter 3345 (Fig. 2) to estimate time of separation as a function of longitude. In most cases, the translation of Loop Current eddies is fairly consistent. Thus, a linear function was used to give time T (days) since eddy separation versus longitude L (degrees west):

$$T = 32.67\ L - 2825.93$$

The results are shown in Fig. 4 which exclude data from the drifter in the Loop Current (Fig. 1) and an additional drifter which was anomalous in that it moved from one eddy to another while in the east-central portion of the GOM. The overall periods of rotation are remarkably consistent during the lifetimes of the eddies (>1 year). Minimum rotation rates are 7 days while maximum rates are 23 days. However, the great majority of the rotation rates are between 9 and 12 days. The variance becomes significant between 175-275 days after eddy separation, a reflection of the increase in rotation rate during the interaction of younger and older eddies (coalescence) in the western Gulf. After these interactions, the rotation rate tends to go back to ~10 days.

The second index is amplitude of the swirl speed versus eddy radius. Fig. 5 is a composite of both east-west and north-south swirl speed amplitudes from all drifters, including the one that was in the Loop Current. Although a distinct trend is seen, the scatter is considerable. However, besides drifter 3354 (which was in the Loop Current), there were several other instances of drifters that were in rather anomalous flow field conditions. For example, drifter 3350 was rather distant from the center of the eddy into which it was seeded (140-150 km) and stopped rotating about the eddy after only 2.5 revolutions. It is unlikely that this drifter was ever really under the influence of the interior flow field of the eddy. Also, drifter 5495 rotated about one eddy for 3-4 revolutions, left that flow field and began rotating around another eddy further to the southwest (Lewis et al., 1989). Again, this drifter was likely not under the direct influence of the core circulation of either eddy. Another drifter, 3344, rotated about one eddy in the central Gulf for quite some time without translating westward. It then surged westward, made three revolutions before finally becoming free of any rotary field of flow. This is one of the more curious drifter trajectories and should be considered quite atypical. Finally, drifter 3378 was seeded in an eddy which moved westward along the northern continental slope of the Gulf (Lewis et al., 1989). Although such a northern path is not unheard of, we will consider it as being abnormal for the determination of swirl speed amplitude versus radius.

After eliminating the above drifters, the composite of speed versus eddy radius shown in Fig. 6 is obtained. The scatter has been reduced considerably, but we note that the scatter for the east-west speeds is substantially less than that for the north-south speeds. Also shown in Fig. 6 is the speed vs. radius profile developed by Cooper et al. (1990) from a variety of velocity measurements from two Loop Current eddies. Our results are quite consistent with their profile, indicating near solid-body rotation out to ~125 km and a maximum speed of a little over 90 cm/s.

The speed vs. radius profiles as determined using the other drifters (3350, 5495, 3344, and 3378) are presented in Fig. 7. These speeds show a distinct tendency to be greater than those shown in Fig. 6 for a given radius.

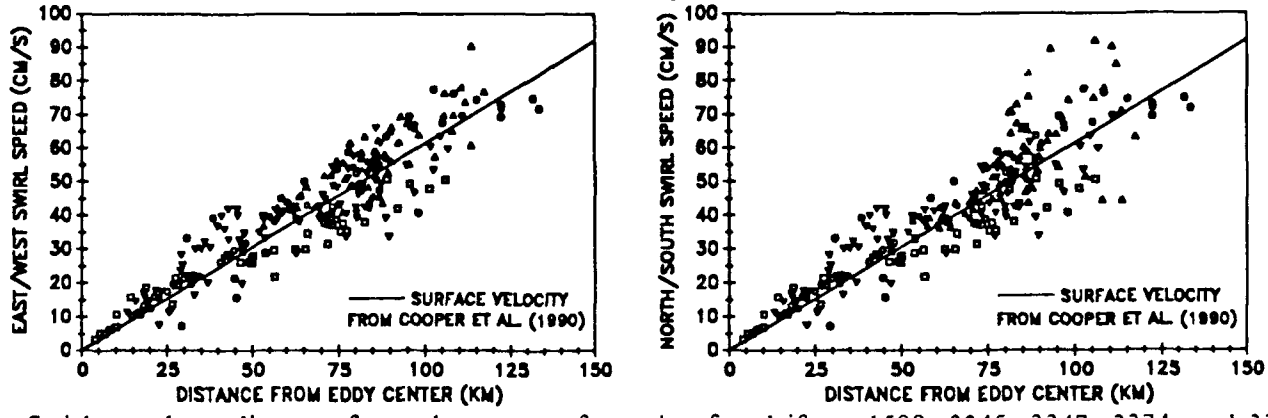

Fig. 6. Swirl speed vs. distance from the center of rotation for drifters 1599, 3345, 3347, 3374, and 3379. The straight line is the horizontal velocity profile for two Loop Current eddies as determined by Cooper et al. (1990).

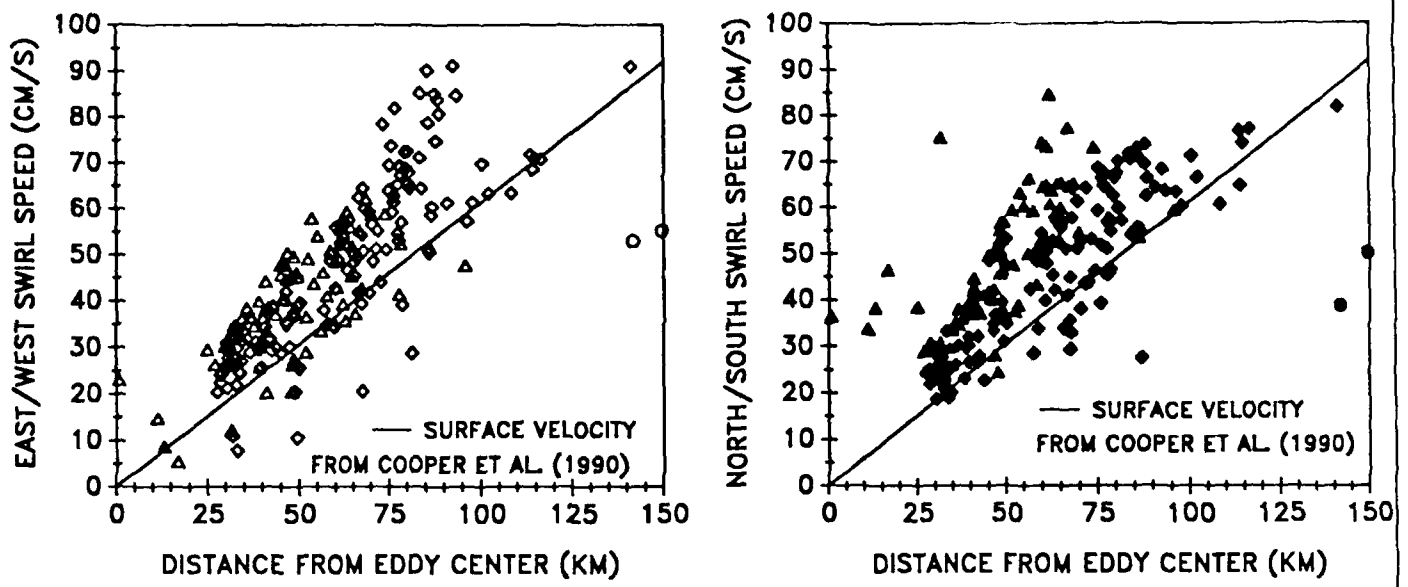

Fig. 7. Swirl speed vs. distance from the center of rotation for drifters 3344, 3350, 3378, and 5495. The straight line is the horizontal velocity profile for two Loop Current eddies as determined by Cooper et al. (1990).

3. ANALYSES OF PATH DATA FROM THE GOM MODEL

The Gulf of Mexico model is based on the formulation of Blumberg and Mellor (1981). It is a sigma-coordinate model which conserves mass, momentum, salt, and heat. The momentum and diffusion equations contain vertical exchange coefficients which are determined by the second-order turbulence closure scheme of Mellor and Yamada (1982). The barotropic and baroclinic modes are split in the model in order to enhance the speed of execution. The model has a 0.2° latitude by 0.2° longitude horizontal resolution, with bathymetry based on data from the National Geophysical Data Center (1985). These bathymetry data are not considered accurate for depths of less than 200 m, so additional data were used to provide a more accurate bathymetry in shallower water. The Gulf model uses the climatological temperature and salinity given by Levitus (1982) for initial conditions.

A computer routine was used to simulate particle trajectories based on the surface current fields of a Loop Current eddy from the model. Path data were analyzed for particles with initial distances from the model eddy center of 25 km out to 130 km. Fig. 8 shows the path of the particle whose initial location was 25 km from the eddy center. As can be seen, the eddy took the more southerly path westward, and the particle remained at approximately the same radial distance for the entire period of the simulation. The velocity components are also shown in Fig. 8 and are of the appropriate magnitude considering the observed speed vs. radius data. However, the velocity data show the trend toward lower magnitudes and longer periods with time. These trends are more readily seen in the kinematic data in Fig. 8 in which we see appropriate translation velocities but slowly decreasing swirl speeds along with an increasing period of rotation. The period of rotation is initially 7 days but increases to 17 days at 175 simulation days. The decreasing swirl magnitudes are not accompanied by a decrease in distance from the eddy center as would be implied by observations.

Another simulated particle trajectory from the same model eddy is shown in Fig. 9. This particle was initially 70 km from the eddy center. The velocity components are also presented, and these begin with a magnitude of ~65 cm/s. This is about 15 cm/s too fast according to the results shown in Fig. 6. These model velocity components again show a decrease in magnitude and increase with period with time (Fig. 9). It should be noted that the period of rotation for this particle is initially greater than the previously discussed particle, and gets as large as 23 days.

4. COMPARISONS AND MODEL ENHANCEMENTS

The analyses of the model trajectory data indicate that the model eddies tend to reproduce observations in terms of the westward and then

northward paths that the eddies take across the GOM. In addition, the model reproduces the translation velocities of actual Loop Current eddies. However, the model eddies do not maintain a consistent period of rotation (within ±3 days) but instead spin down considerably within a period of 7-8 months. This, of course, results in the inability of the model to reproduce observed velocity structures (and, thus, the density fields). We also note that the model trajectories did not show any indication of the model eddy slowly diverging and converging. This slow pumping of the mass field of an eddy was shown by Kirwan and Liu (1991) to be the result of the deformation of the external field of flow in which an eddy is embedded. In the case of the Gulf of Mexico, such deformation is likely induced by the bathymetry of the basin. The GOM model has bathymetry specified at 0.2° intervals of latitude and longitude, and the model eddy should respond appropriately. It is unclear why the model eddy did not pulsate, but it is possible that the routine used to calculate the particle trajectory might be responsible in some way.

The difference between the observed and model eddy kinematics may be the result of several conditions. First, knowledge of the inflow conditions in the Yucatan Straits (salinity, temperature, and velocity structure) has been limited, and the

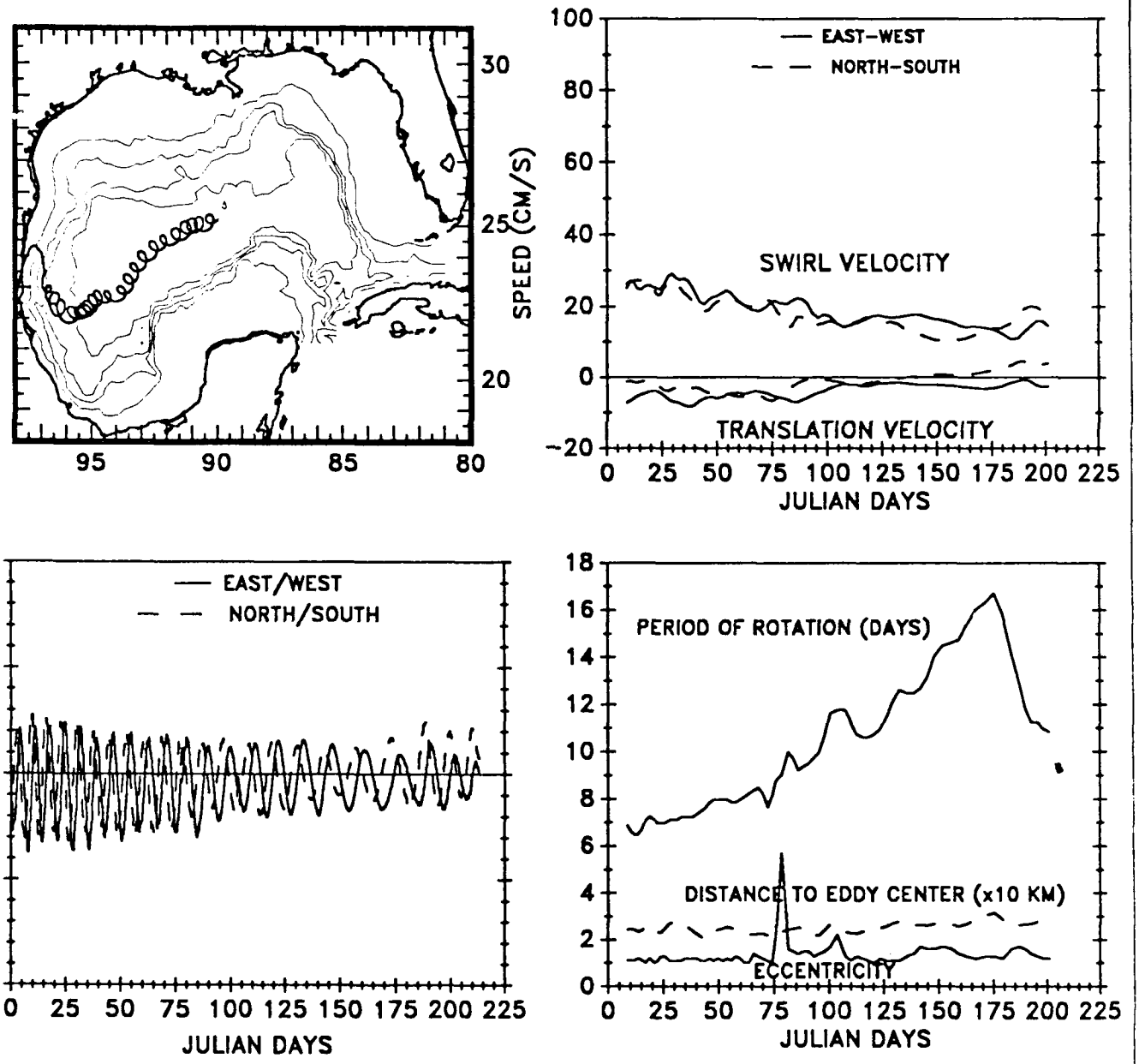

Fig. 8. Trajectory of a particle from a model eddy (top left), the east-west (u) and north-south (v) velocity components (bottom left), swirl and translation velocities (top right) and period of rotation, distance to eddy center, and eccentricity (bottom right).

model specifies only an average current with a 30 Sv flow over the top 1000 m. It is unclear how this approximation affects the results of this particular model, but we can expect at the least unrealistically large turbulence all along the edges of such a flow field. More dramatic effects were found by Sturges et al. (1990). They discovered that a model western boundary current may not even meander, no less shed eddies, with inappropriate inflow conditions. Thus, providing a better approximation of inflow conditions is quite important.

A second factor deals with the horizontal resolution of the model. The radii of ocean eddies vary from 50-100 km. The rule of thumb is that any model grid should be one-tenth of the size of such radii so that appropriate physics will be well defined in the model (Roache, 1976). This implies a horizontal grid resolution of between 5-10 km. The present grid is of the order of 19 km. Moreover, the model formulation is such that the lateral eddy viscosity is related to the lateral grid size. Under this formulation and the present model grid, the lateral viscosity ranges up to a maximum of ~800 m^2/s in high shear regions. According to observations (Bowden, 1962), a smaller value (order of 60 m^2/s) might be more appropriate.

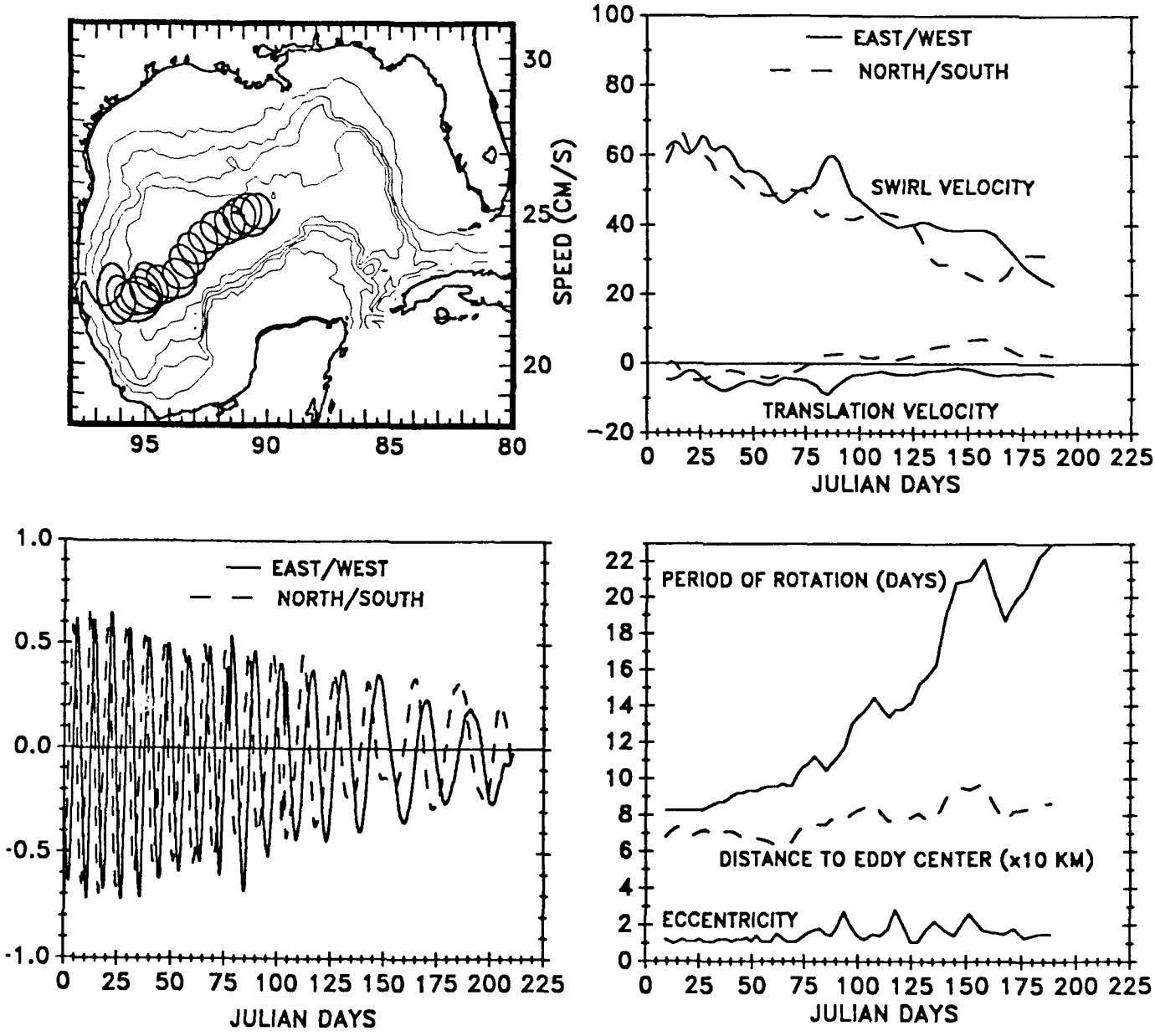

Fig. 9. Same as Fig. 8 but for a particle that was initially 70 km from the center of the model eddy.

It was decided to first develop better inflow conditions for the model and determine how these affect the model eddy kinematics. This was accomplished by the analyses of data from various sources, especially hydrographic data collected in the Yucatan Straits.

Yucatan Straits Inflow Parameters

A variety of data sets were synthesized to produce a depiction of the characteristics of the Gulf Stream as it flows through the Yucatan Straits. These characteristics include the two-dimensional patterns of temperature, salinity, density, and northward velocity as well as the east-west variations of surface height. We started with the work of Cooper et al. (1990) to specify the vertical velocity profile of the Loop Current inflow. Their analyses, based on data from a ring just breaking off from the Loop Current in the eastern Gulf of Mexico, provided a maximum velocity current profile. Cooper et al. found that the structure of the vertical current profile was linearly proportional to the distance from the ring center (i.e., near-solid body rotation). We assumed that flow within the Loop Current would be similar, decreasing linearly to the east and west of the central region of maximum flow. The results of Hall (1989) were used to specify the horizontal structure of the flow field based on the spatial structure of the Gulf Stream in the Atlantic Ocean. The Gulf Stream horizontal flow structure is seen to increase nearly linearly from zero in the west to the maximum velocity some 100 km toward the east. It then decreases further to the east, again almost linearly, to zero flow some 50 km east of the region of maximum velocity. Thus, to specify the surface velocity V_{surf}, we use

$$V_{surf} = \begin{cases} V_{max}\, X/100 & \text{for } 0<X<100 \text{ km} \\ 3V_{max} - V_{max}X/50 & \text{for } 100<X<150 \text{ km} \end{cases}$$

where X is the distance in km from the western edge of the Yucatan Straits and V_{max} is the maximum surface speed of the Loop Current inflow.

The profile (Fig. 10), synthesized over a depth of 800 m and a total width of 150 km, results in a transport of 27.9 Sv. This transport is quite close to the accepted inflow through the Yucatan Straits of 30 Sv. The synthesized profile was adjusted upward to give 30 Sv, an increase of only 7%. The resulting current structure (magnitude with respect to depth) compares well to the limited observations of currents in the Yucatan Straits collected by the Naval Oceanographic Office (unpublished data).

Other inflow parameters required by the model are the horizontal and vertical structure of salinity and temperature. The resulting density field must be consistent with the field of currents. The overall density field was first calculated in a rather simplistic manner, using geostrophy, the synthesized field of currents, and densities along the western boundary of the Yucatan Straits from observations. As it turns out, this approach results in a field of densities that compares favorably with observations in the Yucatan Straits. Inverting the equation of state, we then determined water temperature as a function of density. Once again, this field approximates that from observations. The salinity was then ascertained from the temperature using the T-S relationship for the Yucatan Straits region.

Using the hydrostatic and geostrophic relationships, it can be shown that the density ρ at depth z and distance X from the western edge of the Yucatan Straits is

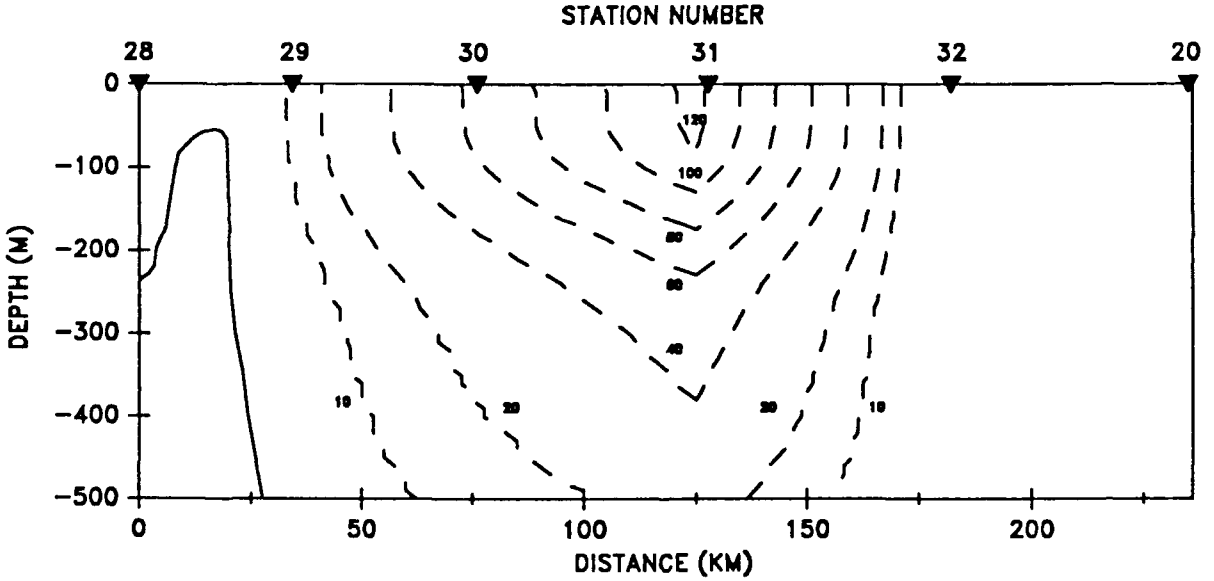

Fig. 10. Synthesized velocity profile (cm/s) of the Gulf Stream within the Yucatan Straits superimposed on the bathymetry at 21°N.

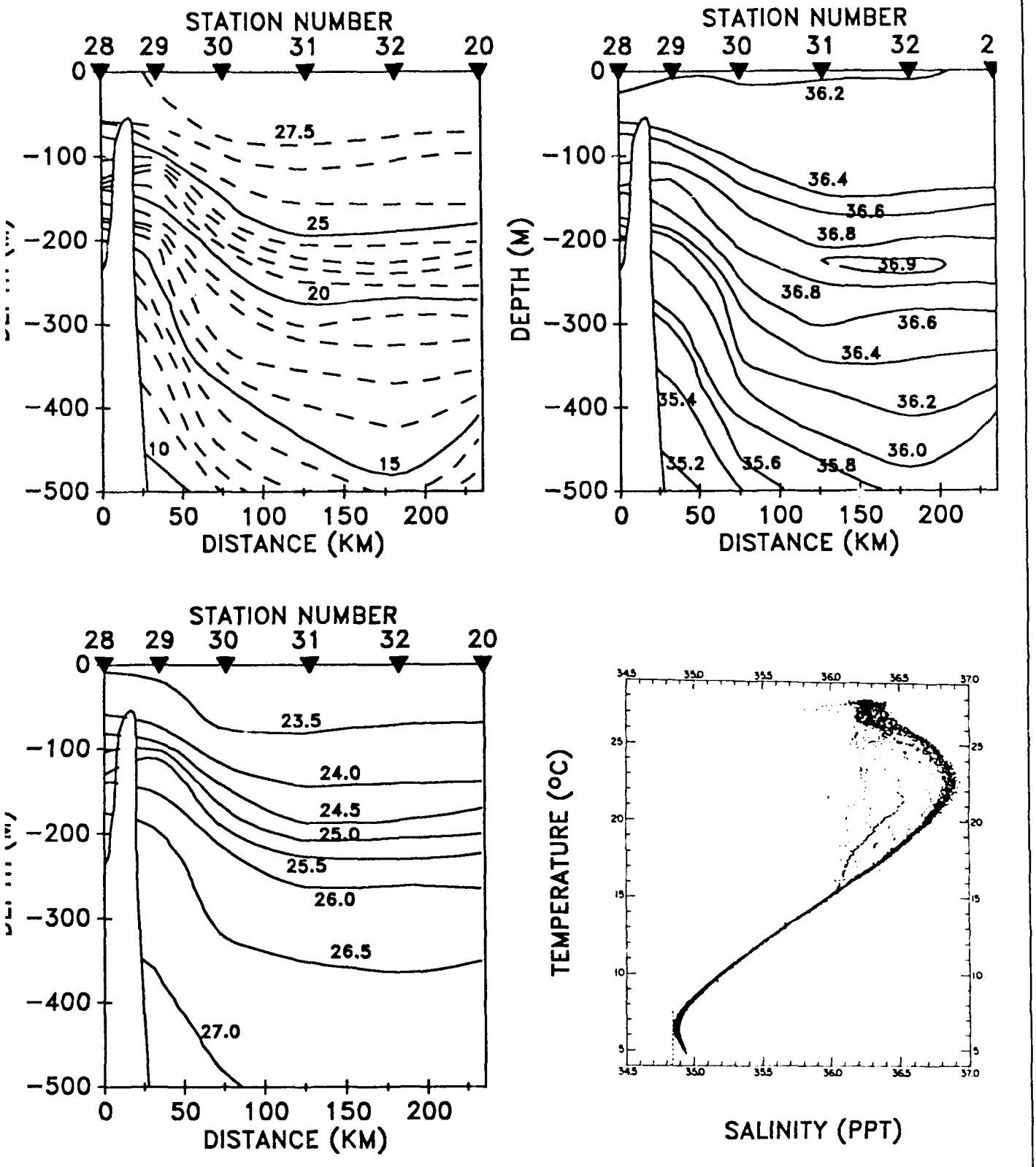

Fig. 11. Observed temperatures (°C), salinities (ppt), and densities (sigma-t) looking northward through the Yucatan Straits at 21°N during 26 May-6 Jun 1984. The T-S diagram reflects all the data collected during the survey.

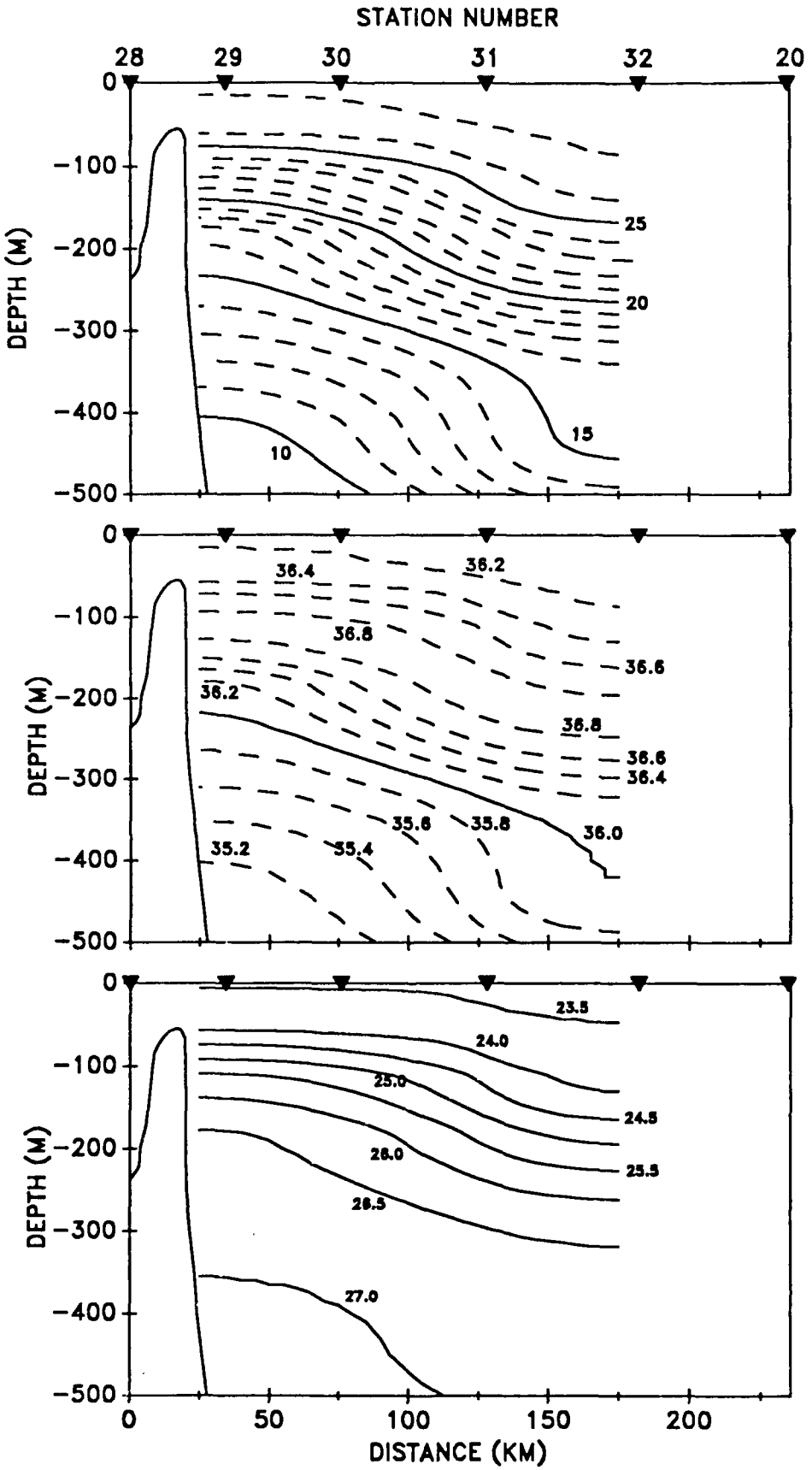

Fig. 12. Synthesized temperatures (top, °C), salinities (middle, ppt), and densities (bottom, sigma-t) looking northward through the Yucatan Straits (superimposed on the bathymetry at 21°N).

$$\rho_{z,X} = \rho_{z,X=0} + \rho_0 f/g \int_0^X \partial V_{x,z}/\partial z \, dx$$

where ρ_0 is an average density (1026.5 kg/m³ for our purposes), $\rho_{z,X=0}$ is the density at depth z along the western boundary of the Yucatan Straits (obtained from observations), f is the Coriolis parameter for 21°N, g is the acceleration of gravity, and $V_{x,z}$ is the synthesized velocity profile. Thus, to obtain the salinity and temperature structures that are consistent with the velocity structure, we require the density information $\rho_{z,X=0}$, a standard equation of state, and a T-S relationship for the Yucatan Straits.

Salinity and temperature data were collected in the region of the Yucatan Straits during 26 May-6 Jun 1984. The temperature, salinity, and density fields along 21°N are shown in Fig. 11. Also shown is the T-S diagram for all the data collected during the survey. The core of the Gulf Stream inflow is contained between stations 29-32, a distance of ~157 km. An additional survey was conducted during November 1989. These data (not shown) show similar salinity and temperature structures but also indicate that the flow field extends down to 800-900 m. Thus, our synthesized flow field matches quite well with the dimensions of the observed flow field.

Using the $\rho_{z,X=0}$ and the T-S relationship as indicated in Fig. 11, we obtained the synthesized density, temperature, and salinity structures as shown in Fig. 12. The density structure is similar to observations, and, as a result, the temperature and salinity structures are also similar to those observed. Since we expect that the inflow is in near-geostrophic balance, these results imply that our synthesized velocity structure is a reasonable approximation to the true flow field in the Yucatan Straits.

A computer routine was generated to calculate the inflow characteristics for a given depth and distance across the Yucatan Straits. This routine is now available to other researchers to aid in specifying appropriate boundary conditions for numerical simulations.

Additional Model Enhancements

Along with the new inflow characteristics, two additional enhancements were made to the model. The first was greater vertical resolution. The original model had 12 sigma-coordinate levels in the vertical, and the new version has 18 levels. This enhanced resolution is not expected to affect the model kinematics.

The second modification is the specification of the outflow conditions through the Florida Straits. In the original model, the outflow parameters were specified as a block transport through a pre-determined region of the open boundary. The hydrographic data collected during the 1989 survey included temperature and salinity structure just west of the Florida Straits at ~82°W. These are shown in Fig. 13. As opposed to using these data to generate a set of synthetic outflow conditions as we did for the Yucatan Straits, it was decided to scale the Yucatan inflow to the Florida Straits. The Yucatan vertically-averaged inflow was adjusted to fit across the deeper portion of the Florida Straits, ~110 km. These new outflows were then increased to match the Yucatan inflows such that mass transport is balanced for each time step of the model in which the barotropic mode is calculated. As for the baroclinic mode, a simple radiation condition was applied at the Florida Straits. In this way, reflection of energy at the Florida Straits should be minimized.

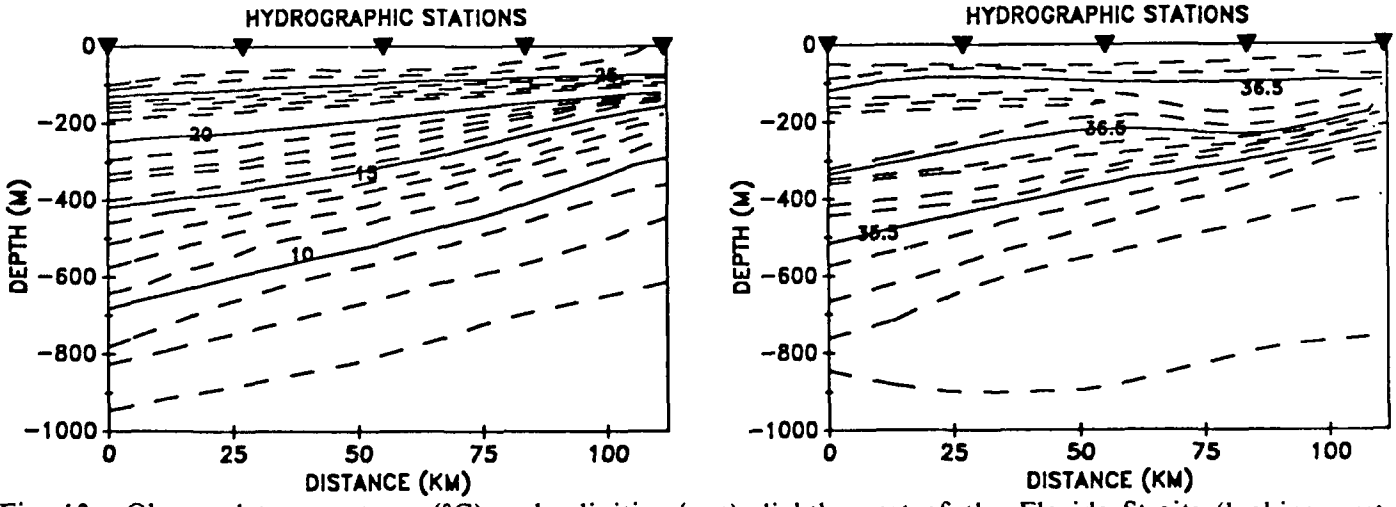

Fig. 13. Observed temperatures (°C) and salinities (ppt) slightly west of the Florida Straits (looking westward) at about 82°W during November 1989.

5. SIMULATIONS TO DATE

The GOM model is now being exercised and tested using the above enhancements. Tests with lower values of lateral eddy viscosities are also being performed. After these tests, simulations will be conducted and we wili recalculate the characteristics of the resulting model eddies. This will allow us to determine the degree of improvement in reproducing the characteristics of observed Loop Current eddies. The outcome of this continued work will be reported as results become available.

ACKNOWLEDGEMENTS

This work was supported by the Institute for Naval Oceanography and the Commander, Naval Oceanography Center.

REFERENCES

Blumberg, A. F., G. L. Mellor, 1981: A description of a three-dimensional coastal ocean circulation model. *Three Dimensional Coastal Models*, Coastal and Estuarine Sciences, 4, N. S. Heaps (ed.), Amer. Geophys. Union Geophysical Monograph Board, 1-16.

Bowden, K. F., 1962: Turbulence. In *The Sea, Vol. 1*, Chap. VI. John Wiley & Sons, New York. 802-825.

Cooper, C., G. Z. Forristall, and T. M. Joyce, 1990: Velocity and hydrographic structure of two Gulf of Mexico warm-core rings. J. Geophys. Res., 95 (C2), 1663-1679.

Hall, M. M., 1989: Velocity and transport structure of the Kuroshio Extension at 35°N, 152°E. J. Geophys. Res., 94 (C10), 14445-14460.

Kirwan, A. D., Jr., W. J. Merrell, Jr., J. K. Lewis, R. E. Whitaker, and R. Legeckis, 1984: A model for the analysis of drifter data with an application to a warm core ring in the Gulf of Mexico. J. Geophys. Res., 89 (C3), 3425-3438.

Kirwan, A. D., Jr., A. W. Indest, Juping Liu, and N. Clark, 1990: Ring Evolution in General Circulation Models from Path Analysis. J. Geophys. Res., 95 (C10), 18057-18073.

Kirwan, A. D., Jr., and Juping Liu, 1991: The role of deformation in the evolution of a non-linear lens. Submitted, Physics of Fluid.

Levitus, 1982: Climatological atlas of the world ocean. NOAA Professional Paper No. 13, U. S. Government Printing Office, Wash. D.C.

Lewis, J. K., and A. D. Kirwan, Jr., 1985. Some observations of ring topography and ring-ring interactions in the Gulf of Mexico. J. Geophys. Res., 90 (C5), 9017-9028.

Lewis, J. K., and A. D. Kirwan, Jr., 1987. Genesis of a Gulf of Mexico ring as determined from kinematic analyses. J. Geophys. Res., 92 (C11), 11727-11740.

Lewis, J. K., A. D. Kirwan, Jr., and G. Z. Forristall, 1989. Evolution of a warm-core ring in the Gulf of Mexico: Lagrangian observations. J. Geophys. Res., 94 (C6), 8163-8178.

Mellor, G. L., and T. Yamada, 1982: A hierarchy of turbulence closer models for planetary boundary layers. J. Atmos. Sci., 31, 1791-1896.

National Geophysical Data Center, 1985: *Worldwide Gridded Bathymetry DBDB5 5-Minute Latitude/Longitude Grid.* Data Announcement 85-MGG-01, NOAA/NGDC, Boulder, CO.

SAIC, 1990: Gulf of Mexico physical oceanography program, final report: Year 5. Vol. II: Tech. Report. OCS Report/MMS - 89-0068, U.S. Dept. of Int., Minerals Management Service, Gulf of Mexico OCS Regional Office, New Orleans, LA. 333 pp.

Roache, P. J., 1976: Computational Fluid Dynamics. Hermosa Publishers, Albuquerque. 446 pp.

Sturges, W., J. C. Evans, S. Welsh, and W. Holland, 1990: The process of ring separation from the Loop Current. Proc., Chapman Conf. On the Physics of the Gulf of Mexico, St. Petersburg Beach, FL, June 1989.

Vukovich, F. M., and P. Hamilton, 1989: New atlas of front locations in the Gulf of Mexico. Proc., MMS Information Transfer Meeting, New Orleans, Dec. 1989.

SAIC

REPORT DOCUMENTATION PAGE

Form Approved
OMB No. 0704-0188

1. Agency Use Only *(Leave blank).*	2. Report Date.	3. Report Type and Dates Covered.
	May 1991	Technical Report, May 1991

4. Title and Subtitle.
"Verification and Calibration of an Eddy-Resolving Model of the Gulf of Mexico"

5. Funding Numbers.
Program Element No. 0601153N
Project No. R310300
Task No. 801
Accession No. DN250022

6. Author(s).
James K. Lewis, Artemio Gallegos, Lakshmi Kantha, Ranjit Passi

7. Performing Organization Name(s) and Address(es).
Science Applications International Corporation
207 S. Seashore Avenue
Long Beach, MS 39560

8. Performing Organization Report Number.
SAIC - 91/1134

9. Sponsoring/Monitoring Agency Name(s) and Address(es).
Naval Oceanographic & Atmospheric Research Laboratory;
Code 110; Stennis Space Center, MS 39529
through
Institute for Naval Oceanography; Bldg. 1103, Rm. 233
Stennis Space Center, MS 39529-5005

10. Sponsoring/Monitoring Agency Report Number.
TR-1

11. Supplementary Notes.
In fulfillment of Subcontract No. S9051 between the Institute for Naval Oceanography and Science Applications International Corporation.

12a. Distribution/Availability Statement.
Approved for Public Release. Distribution is Unlimited.

12b. Distribution Code.

13. Abstract *(Maximum 200 words).*

Techniques for verifying and calibrating an eddy-resolving ocean circulation model have been applied to a model of the Gulf of Mexico (GOM). Various kinematic parameters were calculated using drifter data from GOM Loop Current eddies, and indices of rotational period versus eddy age and swirl velocity versus distance from the eddy center were determined. The observed kinematics were then compared to the same parameters calculated from a model eddy. Although the model can simulate the movement and translation velocities of actual Gulf of Mexico eddies, it does not reproduce the interior flow characteristics of such eddies. In particular, the period of rotation about the center of a model eddy is considerably different from what is observed.

The first attempt at calibrating the model was the development of more realistic inflow conditions in the Yucatan Straits. A variety of data sets were synthesized to produce the two-dimensional distributions of temperature, salinity, density, and northward velocity as well as the east-west variations of surface height. The data of Cooper et al. (1990) was used to specify the vertical velocity profile while the results of Hall (1989) were used to specify the horizontal structure of the flow field.

14. Subject Terms. (U) INO; (U) PEDAM; (U) OGCMm; (U) Eddy-Resolving Models; (U) Calibration; (U) Ocean Eddies (U) Yucatan Straits

15. Number of Pages. 14

16. Price Code.

17. Security Classification of Report.	18. Security Classification of This Page.	19. Security Classification of Abstract.	20. Limitation of Abstract.
Unclassified	Unclassified	Unclassified	SAR